The histone H3.3K27M mutation in pediatric glioma reprograms H3K27 methylation and gene expression

Kui-Ming Chan,[1,5] Dong Fang,[1,5] Haiyun Gan,[1] Rintaro Hashizume,[2] Chuanhe Yu,[1] Mark Schroeder,[3] Nalin Gupta,[2] Sabine Mueller,[2] C. David James,[2] Robert Jenkins,[4] Jann Sarkaria,[3] and Zhiguo Zhang[1,6]

[1]Department of Biochemistry and Molecular Biology, [2]Department of Neurological Surgery, University of California at San Francisco, San Francisco, California 94143, USA; [3]Department of Radiation Oncology, [4]Department of Laboratory Medicine Pathology, Mayo Clinic, Rochester, Minnesota 55905, USA

Recent studies have identified a Lys 27-to-methionine (K27M) mutation at one allele of *H3F3A*, one of the two genes encoding histone H3 variant H3.3, in 60% of high-grade pediatric glioma cases. The median survival of this group of patients after diagnosis is ~1 yr. Here we show that the levels of H3K27 di- and trimethylation (H3K27me2 and H3K27me3) are reduced globally in H3.3K27M patient samples due to the expression of the H3.3K27M mutant allele. Remarkably, we also observed that H3K27me3 and Ezh2 (the catalytic subunit of H3K27 methyltransferase) at chromatin are dramatically increased locally at hundreds of gene loci in H3.3K27M patient cells. Moreover, the gain of H3K27me3 and Ezh2 at gene promoters alters the expression of genes that are associated with various cancer pathways. These results indicate that H3.3K27M mutation reprograms epigenetic landscape and gene expression, which may drive tumorigenesis.

Supplemental material is available for this article.

Received March 13, 2013; revised version accepted April 1, 2013.

Malignant gliomas, including glioblastoma multiforme (GBM) and diffuse intrinsic pontine glioma (DIPG), are the most aggressive primary malignant brain tumors in adults and children (Wong et al. 1999; Buckner 2003; Louis et al. 2007). Recent studies have identified somatic mutation of the *H3F3A* gene that encodes the histone H3 variant H3.3 and results in a Lys 27-to-methionine change in the encoded protein (H3.3K27M) (Schwartzentruber et al. 2012; Sturm et al. 2012; Wu et al. 2012) in 60% of DIPG. The median survival of this group of patients after diagnosis is ~1 yr, with no cure in sight. In human cells, unlike canonical histone H3 proteins (H3.1/H3.2) that are encoded by 13 distinct genes, there are two genes encoding histone H3.3 (Henikoff and Ahmad 2005; Ransom et al. 2010; Szenker et al. 2011). H3K27 is conserved among all histone H3 proteins—both canonical histone H3 and its variant, H3.3. Thus, the mechanism by which mutating one allele of the two H3.3 genes drives tumorigenesis is largely unknown.

Histone proteins are modified post-translationally, and these modifications include acetylation, methylation, ubiquitylation, and phosphorylation (Strahl and Allis 2000; Zhang and Reinberg 2001; Li et al. 2007). Both acetylation and methylation have been detected on H3K27. H3K27 acetylation and trimethylation (H3K27ac and H3K27me3) mark distinct chromatin regions and have distinct functions. For instance, in yeast cells, H3K27ac, catalyzed by both Gcn5 and Rtt109 lysine acetyltransferases, is likely to occur on newly synthesized histone H3 (Burgess et al. 2010). In human cells, H3K27ac, in combination with other histone marks, including H3K4me1, marks gene enhancers (Heintzman et al. 2009). H3K27me3, catalyzed by the Polycomb-repressive complex 2 (PRC2) methyltransferase, is enriched at silent gene promoters in mammalian cells (Bernstein et al. 2006; Barski et al. 2007) as well as inactivated X chromosomes in female mammals (Plath et al. 2003) and plays an important role in regulating expression of developmentally regulated genes (Zhang and Reinberg 2001; Simon and Kingston 2009; Margueron and Reinberg 2011). H3K27me3 is also found at "bivalent chromatin domains" that contain active H3K4me3 (Bernstein et al. 2006; Barski et al. 2007). The expression of genes with bivalent marks in general is low and is poised for rapid changes in gene expression during development.

Because of the critical functions of H3K27 methylation and acetylation, we analyzed to what extent H3K27ac and H3K27me2 (H3K27dimethylation)/me3 were altered in cancer cells harboring H3.3K27M mutation. Surprisingly, we observed a global reduction in the levels of H3K27me2/me3, but not H3K27ac, in two DIPG cancer lines compared with human neural stem cells (NSCs). This reduction is most likely due to expression of H3.3K27M mutant proteins, since expression of a H3.3K27M transgene in three different cell types resulted in a global reduction in H3K27me2/me3 levels. In addition, we also observed a significant gain of H3K27me3 and Ezh2 locally at hundreds of chromatin loci. Gene expression analysis indicates that genes with a gain of H3K27me3 exhibited reduced expression compared with NSCs and were associated with cancer pathways. Together, our data demonstrate that H3.3K27M mutation dominantly reprograms the epigenetic landscape and gene expression, which may contribute to carcinogenesis.

Results and Discussion

Methylation and acetylation of histone H3 at Lys 27 regulate gene expression (Zhang and Reinberg 2001; Simon and Kingston 2009; Margueron and Reinberg 2011). To gain insight into the impact of H3.3K27M mutation, tumor tissues containing the heterozygous mutation of *H3F3A* from two H3.3K27M DIPG patients (SF7761 and SF8628) were isolated (Supplemental Fig. 1A; Hashizume et al. 2012), and cells were cultured in vitro. These cells formed neural spheres and expressed the NSC marker

[*Keywords*: H3.3K27M; H3K27 methylation; PRC2; gliomas; pediatric]
[5]These authors contribute equally to this work.
[6]Corresponding author
E-mail: zhang.zhiguo@mayo.edu
Article published online ahead of print. Article and publication date are online at http://www.genesdev.org/cgi/doi/10.1101/gad.217778.113.

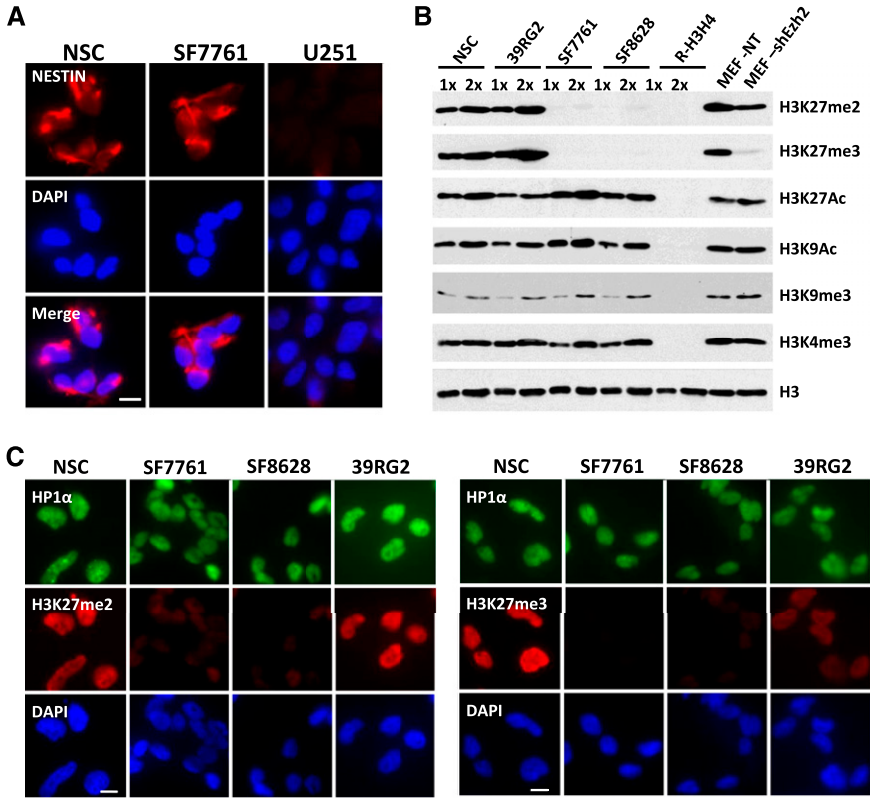

Figure 1. Histone H3K27me2 and H3K27me3 are altered in pediatric DIPG "Histone H3.3 K27M" patient cells. (*A*) NSC marker NESTIN is expressed in human NSCs and in a xenograft from Histone H3.3 K27M patient DIPG cells (SF7761) but not in cells from a human glioblastoma line with a wild-type histone H3.3 (U251). (*B*) Histone H3K27 methylation is specifically altered in H3.3K27M cells. Recombinant histone H3–H4 proteins purified from bacteria (R-H3H4) served as a control to show the specificity of antibodies against modified histone H3 variants. Lysates from mouse embryonic fibroblasts (MEFs) infected with nontargeting (NT) control and Ezh2 shRNA knockdown viruses were used to demonstrate the specificity of the H3K27me2 and H3K27me3 antibodies. (*C*) H3K27me2 and H3K27me3 are reduced in two H3.3K27M patient lines but not in adult GBM, as indicated by immunofluorescence staining. Bar, 5 μm.

Nestin (Fig. 1A; data not shown). We analyzed the histone modifications in these two H3.3K27M tumor lines, a differentiation state-matched NSC line (Fig. 1A), and one adult GBM line (39RG2). H3K27me2 and H3K27me3 were dramatically reduced in the two patient lines compared with NSCs or the adult GBM xenograft line as detected by Western blot (Fig. 1B) and immunofluorescence (Fig. 1C). In contrast, the levels of H3K27ac and other marks on histone H3, such as H3K9me3 and H3K4me3, were not altered to a detectable degree (Fig. 1B). Furthermore, the levels of HP1α, the H3K9me3 reader, and Suz12 and Ezh2, two subunits of the PRC2 complex (Simon and Kingston 2009; Margueron and Reinberg 2011; Yang et al. 2012), were not altered significantly in these cells (Fig. 1B; Supplemental Fig. 1B). Together, these results reveal that the levels of H3K27me2/me3 are reduced in the H3.3K27M tumor cells, and the reduction is not due to a reduced level of Ezh2 or the PRC2 complex.

To determine whether H3.3K27M mutation is the cause of global reduction in H3K27me2 and H3K27me3, we established 293T cell lines expressing low levels of H3.3K27M (less than one-tenth of endogenous of H3). As controls, we also established stable lines expressing H3.1K27M, H3.1/H3.3K27R, and H3.1/H3.3G34R. The H3.3G34R mutation is frequently found in GBM, and this G34R mutation appears to be mutually exclusive from the K27M in GBM tumors (Sturm et al. 2012). As shown in Figure 2A and Supplemental Figure 1C, H3K27me2 and H3K27me3 were dramatically reduced in cells expressing the H3.1K27M or H3.3K27M transgene but not in cells expressing H3.1/H3.3K27R or H3.1/H3.3 G34R mutant proteins. Moreover, the dramatic reduction in H3K27me2/me3 was also observed in human astrocytes (Fig. 2B) and mouse embryonic fibroblasts (MEFs) expressing the H3K27M mutant proteins (Fig. 2C). These results demonstrate that the expression of H3.1 or H3.1 K27M mutant proteins reduce the endogenous H3K27me2/me3 in a cell type-independent manner and explain the global reduction in H3K27me2/me3 observed in H3.3K27M DIPG patient cells. Furthermore, we found that the di- and trimethylation of H3K36 is reduced on the ectopically expressed Flag-H3.3G34R but not the endogenous histone H3 (Supplemental Fig. 2), suggesting that the glycine residues at position 34 are important for the di- and trimethylation of Lys 36.

Examination of the H3K27me2/me3 levels by immunofluorescence revealed that cells stably expressing K27M mutant proteins exhibited a reduction in H3K27 methylation in the whole population (Supplemental Figs. 3, 4). To investigate the temporal effect of H3K27M mutant proteins on endogenous H3K27me3, we transiently transfected the Flag-H3.1/H3.3K27M transgene into MEF cells and monitored the H3K27me3 level using fluorescence microscopy (Fig. 2D). We did not observe significant

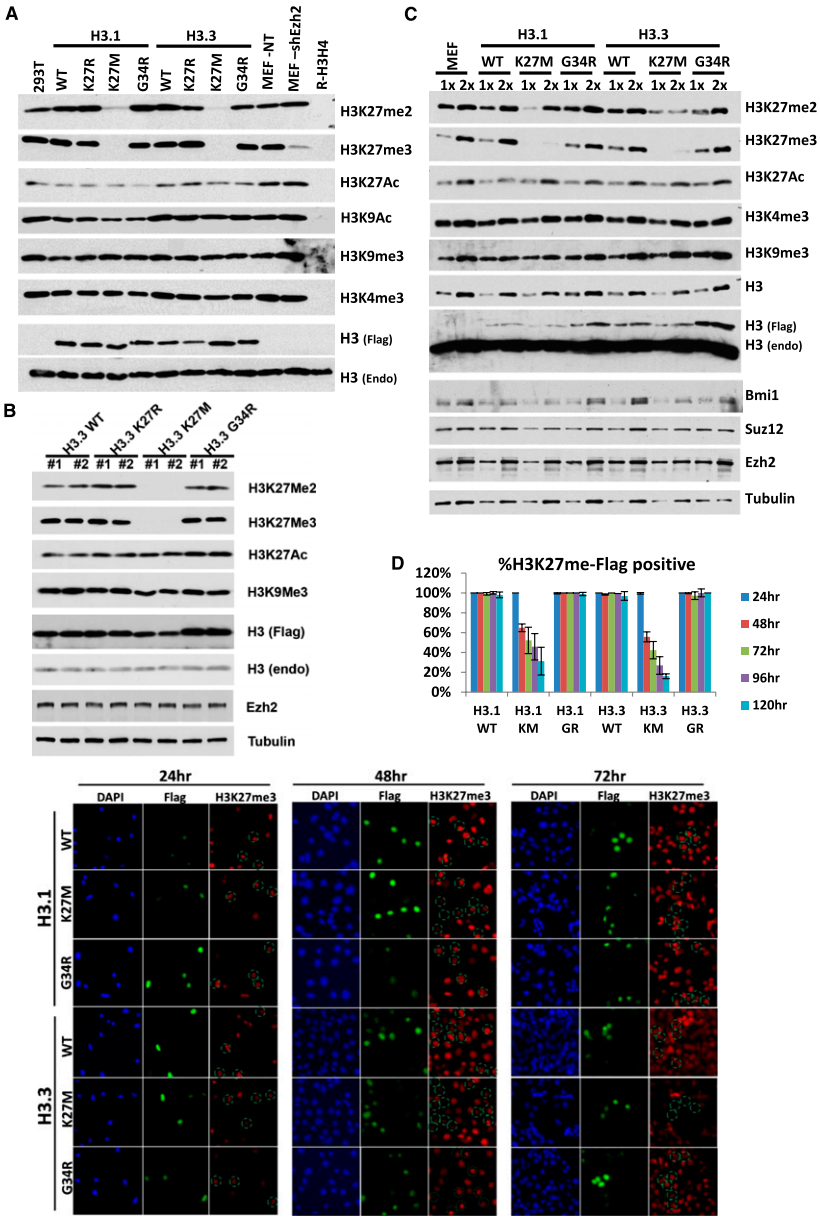

Figure 2. Ectopic expression of Histone H3.1 and H3.3 K27M mutants alters endogenous histone H3K27 methylation. (*A*) Lysates collected from individual 293T clones stably expressing Flag-tagged wild-type (WT) human histone H3.1 and H3.3 or mutant (K27R, K27M, or G34R) histone proteins were subjected to Western blotting. Recombinant histone (R-H3–H4) purified from bacteria and lysates from MEFs infected with Ezh2 shRNA served as controls to show the specificity of the antibodies. (*B*) H3.3K27M mutant histones alter endogenous H3K27me2 and H3K27me3 in human astrocyte cell lines. Two individual clones were analyzed. The experiments were performed as described in *A*. (*C*) H3.1 and H3.3 K27M mutant histones specifically alter endogenous H3K27me2 and H3K27me3 in MEF cells. Lysates from individual stable clones were collected and subjected to Western blotting. (*D*) Loss of H3K27me3 in MEF cells expressing histone H3.1 or H3.3 K27M mutant proteins is gradual. Immunofluorescence photographs of Flag-tagged wild-type or mutant histone H3.1 and H3.3 proteins expressed in MEF cells and monitored over time for changes in H3K27me3. The corresponding bar chart shows the percentage of wild-type H3 or H3 mutant-expressing cells with H3K27me3 staining. Results were averaged from two independent experiments ($n > 200$). Bar, 5 μm.

changes in H3K27me3 in cells expressing H3.1/H3.3K27M 24 h after transfection. In contrast, ~40% of H3K27M-expressing cells exhibited reduced H3K27me3 staining 48 h after transfection. The percentage of cells that retained H3K27me3 continued to decrease in a time-course experiment (70%–80% 120 h post-transfection). These results suggest that it takes multiple cell divisions for the H3K27M mutant proteins to exert their full effect on H3K27 methylation.

Next, we investigated the genomic distribution of H3K27me3, H3K4me3, and Ezh2 in NSCs and cancer line SF7761 cells using chromatin immunoprecipitation (ChIP) coupled with next-generation sequencing (ChIP-seq) (Fig. 3A; Barski et al. 2007). Using SICER software (Zang et al. 2009), we identified a total of 17,711 peaks in NSCs (P-value < 10^{-6}; false discovery rate [FDR] < 0.01). These H3K27me3 peaks are associated with 5718 RefSeq genes, with 3912 located at the promoters and 1806 located within the gene body. In contrast, we identified 2684 peaks in SF7761 cells with the same cutoff values. Compared with NSCs, the reduction in H3K27me3 peak number in SF7761 was observed in all gene elements examined (promoters, exons, introns, 5′ and 3′ untranslated regions [UTRs], and intergenic regions) (Fig. 3B), and the normalized H3K27me3 tag density in the gene body was significantly reduced (Fig. 3C). Meanwhile, we did not detect dramatic changes in the number of H3K4me3 or Ezh2 peaks between SF7761 cells and NSCs (Fig. 3B,C). Together, these ChIP-seq results strongly suggest that the overall chromatin-associated H3K27me3 is dramatically reduced in SF7761 cells compared with NSCs.

H3K27me3 peaks detected in SF7761 cells spanned a larger chromatin region than those found in NSCs (Supplemental Fig. 5). Of the 2684 H3K27me3 peaks detected in SF7761 cells, 63% were unique to this cancer line in relation to NSCs. Surprisingly, these unique peaks had significantly more tagged density than corresponding peaks found in NSCs (Fig. 3A,D). These results indicate that the level of H3K27me3 at these loci, such as the long isoform of CDK6, is significantly elevated compared with NSCs (Fig. 3D). The increase in H3K27me3 at the long isoform, but not the short isoform, of CDK6 was confirmed by ChIP and quantitative real-time PCR in two H3.3K27M patient samples (Fig. 3E). As a control, we also tested the OLIG2 loci showing a significant decrease of H3K27me3 (Fig. 3D,E). Finally, peaks unique to SF7761 cells overlapped completely with Ezh2 peaks, and 81% of all H3K27me3 peaks overlapped with Ezh2 peaks in SF7761 cells, compared with just 9% in NSCs (Supplemental Fig. 5). Since Ezh2 is the catalytic subunit of the PRC2 complex responsible for the methylation of histone H3 at Lys 27, our results suggest that the gained H3K27me3 peaks in SF7761

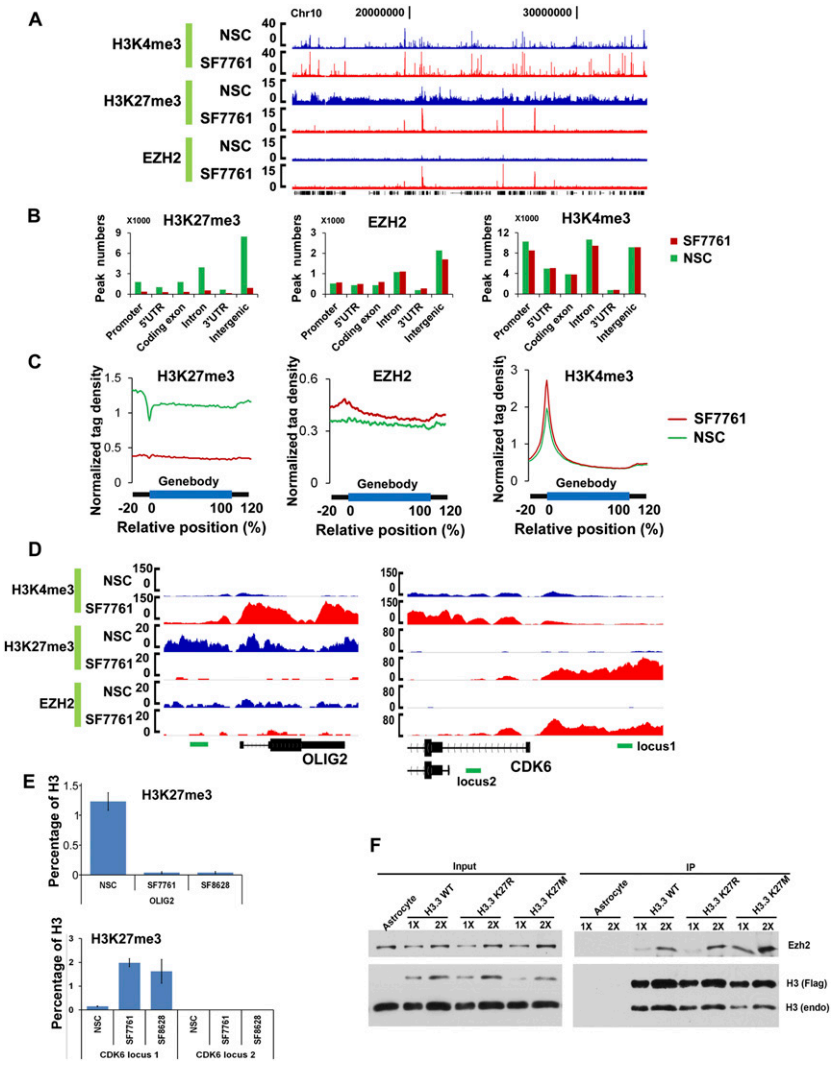

Figure 3. Genome-wide mapping of H3K4me3, H3K27me3, and EZH2 in NSCs and SF7761 (H3.3K27M DIPG patient). (*A*) The distribution of H3K4me3, H3K27me3, and EZH2 in the region of chromosomes 10:21,243,862–31,717,550. RefSeq genes are shown at the *bottom*. (*B*) H3K4me3, H3K27me3, and EZH2 gene structural element associations in NSCs (green) and SF7761 cells (red). Promoters were defined as −2 kb to +1 kb relative to transcription start site (TSS). (*C*) Normalized tag distribution profiles of H3K4me3, H3K27me3, and EZH2 peaks across gene body regions. Each gene body was normalized to 0%–100%, with 20% upstream of and 20% downstream from the gene body shown. (*D*) Genome browser track examples for the occupancy profiles of two genes: OLIG2 and CKD6. (*E*) ChIP-qPCR analysis to validate the H3K27me3 ChIP-seq results at the OLIG2 and CDK6 loci. (*F*) Ezh2 copurifies to a greater extent with exogenously expressed H3.3 K27M than with H3.3 wild type (WT) and K27R in vivo. H3.3 mononucleosomes were immunoprecipitated from astrocyte cells stably expressing the Flag-tagged H3.3 K27M mutant. The same purification procedures were performed using normal astrocytes as a negative control. Proteins in whole-cell extracts (Input) and immunoprecipitates (IP) were analyzed by Western blotting using the indicated antibodies.

could be the consequence of the enriched occupancy of Ezh2 at those loci.

To determine whether the gained overlap peaks of Ezh2 and H3K27me3 detected in SF7761 cells is linked to H3.3K27M mutation, we immunoprecipitated mononucleosomes from cells exogenously expressing Flag-tagged wild-type H3.3, H3.3K27R, and H3.3K27M and detected Ezh2 by Western blot (Fig. 3F). A marked increase in Ezh2 was detected on mononucleosomes copurified with H3.3K27M compared with H3.3 or H3.3K27R. These results strongly suggest that the increase in H3K27 methylation at unique loci in SF7761 cells is due to the recruitment/retention of Ezh2 in the presence of H3.3K27M mutant protein.

We classified genes with loss of H3K27me3 in SF7761 cells compared with NSCs as group A genes and those with gain of H3K27me3 as group C genes (Fig. 4A). Analysis of H3K4me3 density at the gene promoter revealed that group A genes had a higher H3K4me3 density at the gene promoters (Supplemental Fig. 6). In contrast, H3K4me3 density at the gene promoter was not altered to a significant degree in group B genes, where H3K27me3 peaks were common to SF7761 and NSCs. Remarkably, H3K4me3 was also detected at gene promoters of the group C genes with significant gain of H3K27me3 (Supplemental Fig. 6). These results indicate that group C genes behave like "bivalent" genes, containing both active H3K4me3 and repressive H3K27me3 marks (Bernstein et al. 2006).

To determine the extent to which genomic changes in H3K27me3 location affected gene expression, we analyzed gene expression profiles in NSCs and two H3.3K27M cancer lines using RNA sequencing (RNA-seq). We observed that the average expression of the 2975 group A genes was higher in both tumor lines compared with NSCs. In contrast, the average expression of group C genes was significantly lower in both cancer lines than in NSCs (Fig. 4B). Figure 4C shows RNA-seq results of OLIG2 (a group A gene) and CDK6 (a group C gene). Using quantitative RT–PCR (qRT–PCR), we validated that the expression levels of OLIG2 in two cancer lines was higher than those in NSCs. Similarly, the expression of the long isoform of CDK6 (NM_001259) was significantly lower in both H3.3K27M patient lines relative to NSCs. In contrast, the expression of the short form of CDK6 (NM_001145306), in which no gain of H3K27me3 peak was detected by ChIP-seq (Fig. 3D), was not altered in DIPG patient cells (Fig. 4D). Kyoto Encyclopedia of Genes and Genomics (KEGG) pathway enrichment analysis indicated that group A genes were associated with various neurological processes, including neuroactive ligand–receptor interactions (P-value = 5.9×10^{-22}), cell–cell signaling (P-value = 6.6×10^{-17}), gated channel activity (P-value = 2.1×10^{-15}), and synaptic transmission (P-value = 6.7×10^{-15}) (Fig. 4E). Gene ontology (GO) and KEGG pathway analyses for the 775 group C genes showed that these are involved in pathways in cancer (P-value 9.0×10^{-6}), embryonic morphogenesis (P-value = 1.7×10^{-5}), transcription

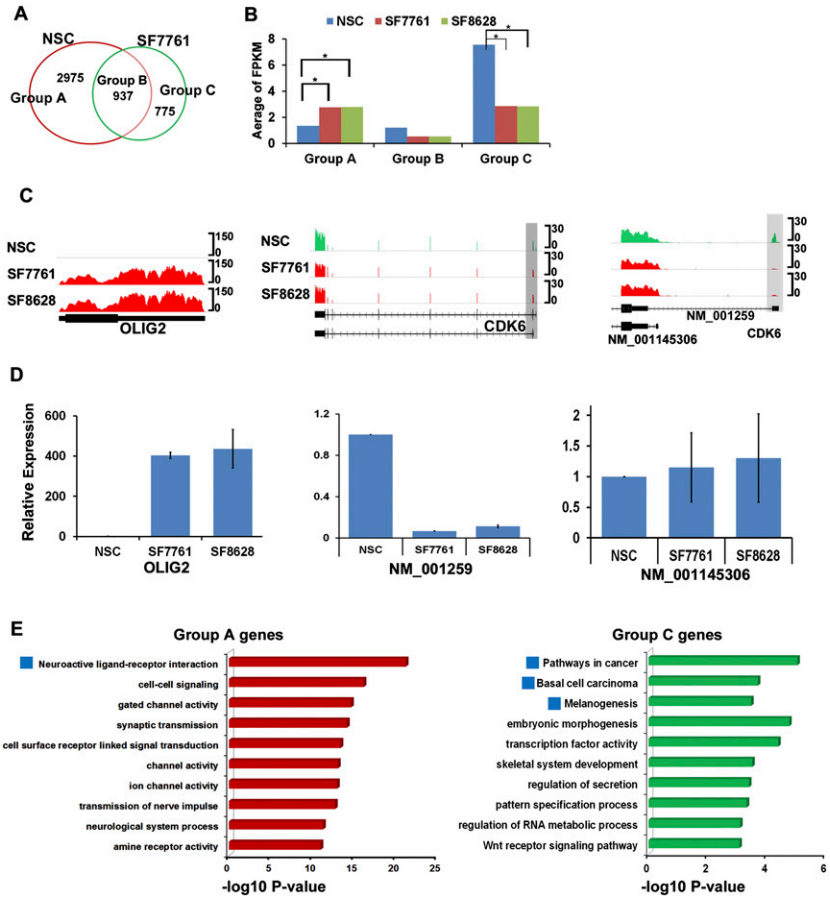

Figure 4. Whole-genome changes in H3K27me3 chromatin association in H3.3K27M DIPG affects gene expression. (*A*) Venn diagram showing the extent of overlap between the genes with H3K27me3 at the promoters in NSCs versus SF6671 cells. Promoters were defined as −2 kb to +1 kb relative to the TSS. From these results, genes were classified into three groups according to promoter occupancy of H3K27me3 in NSC versus SF7761. Group A genes exhibited H3K27me3 peaks only in NSCs, group B genes showed H3K27me3 peaks in both NSCs and SF7761 cells, and group C genes showed H3K27me3 peaks only in SF7761 cells. (*B*) Average expression for each of the three groups of genes. SF8628 is another DIPG patient line containing the H3.3K27M mutation. FPKM (fragments per kilobase of exon per million fragments mapped) was calculated by using Cufflinks software. (*) $P < 0.01$. (*C*) Genome browser track examples of OLIG2 and CKD6 from RNA-seq analysis. CDK6 has two isoforms (NM_001259 and NM_001145306) with the different promoters. The gain in H3K27me3 peaks at the NM_001145306 promoter reduces the expression of this isoform. Also see the Supplemental Material. (*D*) qRT–PCR analysis to validate the RNA-seq data. OLIG2 expression is dramatically elevated in the two H3.3K27M patient cell lines. Expression of the long isoform (NM_001259) of CDK6 was decreased in the two H3.3K27M patient cell lines, while the short isoform (NM_001145306) was unaffected compared with NSCs. (*E*) The GO pathway analysis results for group A and group C genes are shown. KEGG pathway results in agreement with GO pathway results are indicated by blue squares.

factor activity (P-value = 4.0×10^{-5}), basal cell carcinoma (P-value = 2×10^{-5}), and melanogenesis associations (P-value = 1.9×10^{-4}). These results reveal that alterations in the H3K27me3 genomic pattern in H3.3K27M cancer cells affect gene expression.

The H3.3K27M mutation is detected frequently in pediatric DIPG but not in adult GBM cases. The absence of H3.3K27M mutation in adult GBM cases suggests that H3.3K27M mutation might promote tumorigenesis in NSCs or neural precursor cells during early brain development. We acknowledged that the NSCs used for the ChIP-seq and RNA-seq experiments may not be the perfect control for the DIPG patient cells despite being maintained in a neuronal lineage-committed stem cell state (NESTIN expression in Fig. 1A; data not shown). For this reason, ChIP-seq analysis of neuronal cells expressing tagged H3.3 wild-type and H3.3K27M mutant histones would greatly consolidate the data on the recruitment/retention of Ezh2 by H3.3K27M mutant in vivo and eliminate the concern on the choice of proper controls.

Our genome-wide sequencing data suggest that rewiring of H3K27me2/me3 at chromatin, including both loss and gain of H3K27me3 by the H3.3K27M mutation, is likely the primary driver for tumor formation of pediatric DIPG. Our results show that genes with gain of H3K27 methylation are associated with tumorigenesis. Indeed, *p16Ink4A*, a known tumor suppressor, is one of the group C genes, and the expression is dramatically reduced in the two DIPG cell lines by RNA-seq (data not shown). It would be interesting to determine whether re-expression of this group of genes using inhibitors against Ezh2 or histone deacetylases will be beneficial to the treatment of H3.3K27M tumor patients (Dokmanovic et al. 2007; McCabe et al. 2012). In addition to H3.3K27M mutation, H3.3 is also mutated at G34, and mutant H3.3G34R/V is found in a subgroup of pediatric GBM patients. Our results show that exogenous expression of H3.3G34R does not have an apparent effect on endogenous H3K27/H3K36 methylation and are consistent with the idea that H3.3G34R/V promotes tumorigenesis through a distinct mechanism. In the future, it would be interesting to determine how the H3.3G34R mutation affects the epigenetic landscape and gene expression in DIPG tumor cells.

Materials and methods

Cell culture

SF7761 and SF8628 cell lines from patients harboring the histone H3.3 K27M mutation were obtained from Hashizume et al. (2012). NSCs (N7800-100) were purchased from Invitrogen and cultured and maintained in NSC medium (A10509-01, StemPro NSC SFM, Invitrogen). Female immortalized MEF cells have been described (Chan et al. 2011; Chan and Zhang 2012). 293T and human astrocytes were cultured under standard conditions.

ChIP-seq

ChIP was performed the same way as ChIP assay, except that DNA was recovered from the protein G complex using elution buffer (10 mM Tris at pH 8.0, 10 mM EDTA at pH 8.0, 1% SDS, 150 mM NaCL, 5 mM DTT). DNA was subsequently purified using Qiagen Mini Elute PCR purification kit. The ChIP DNA libraries were prepared with the Ovation Ultralow DR Multiplex system (NuGEN). The ChIP-seq libraries were

analyzed by Solexa/Illumina high-throughput sequencing. Reads were aligned to the human genome (hg19) using the Bowtie (Langmead et al. 2009) software using the preset parameters. Only uniquely mapping reads were used for the further analysis. The average coverage in each base pair was computed across the genome and rendered in the Integrative Genomics Viewer. Peak detection was done using MACS (Feng et al. 2012) for H3K4me3 and using SICER (Zang et al. 2009) for H3K27me3 and EZH2. For the H3K4me3 peak, we used *P*-value < 1×10^{-6}. For the H3K27me3 and EZH2 peak, we used *P*-value < 1×10^{-6} and FDR <0.01, window size of 200, and gap size of 600. The genomic features used for the annotation were the peaks obtained from University of California at Santa Cruz Tables tools (hg19) that only RefSeq mRNA used. The peaks were assigned to a given genomic feature if the summit of the peaks overlapped. KEGG pathway and GO term analyses were performed with DAVID (Dennis et al. 2003) databases.

Other materials and methods used in this study are described in the Supplemental Material.

Acknowledgments

We thank Stephanie Safgren for performing immunofluorescence of Nestin. This work is supported by grants from the NIH (CA157489 and GM99722) and the Pediatric Brain Tumor Foundation.

References

Barski A, Cuddapah S, Cui K, Roh TY, Schones DE, Wang Z, Wei G, Chepelev I, Zhao K. 2007. High-resolution profiling of histone methylations in the human genome. *Cell* **129:** 823–837.

Bernstein BE, Mikkelsen TS, Xie X, Kamal M, Huebert DJ, Cuff J, Fry B, Meissner A, Wernig M, Plath K, et al. 2006. A bivalent chromatin structure marks key developmental genes in embryonic stem cells. *Cell* **125:** 315–326.

Buckner JC. 2003. Factors influencing survival in high-grade gliomas. *Semin Oncol* **30:** 10–14.

Burgess RJ, Zhou H, Han J, Zhang Z. 2010. A role for Gcn5 in replication-coupled nucleosome assembly. *Mol Cell* **37:** 469–480.

Chan KM, Zhang Z. 2012. Leucine-rich repeat and WD repeat-containing protein 1 is recruited to pericentric heterochromatin by trimethylated lysine 9 of histone H3 and maintains heterochromatin silencing. *J Biol Chem* **287:** 15024–15033.

Chan KM, Zhang H, Malureanu L, van Deursen J, Zhang Z. 2011. Diverse factors are involved in maintaining X chromosome inactivation. *Proc Natl Acad Sci* **108:** 16699–16704.

Dennis G Jr, Sherman BT, Hosack DA, Yang J, Gao W, Lane HC, Lempicki RA. 2003. DAVID: Database for Annotation, Visualization, and Integrated Discovery. *Genome Biol* **4:** 3.

Dokmanovic M, Clarke C, Marks PA. 2007. Histone deacetylase inhibitors: Overview and perspectives. *Mol Cancer Res* **5:** 981–989.

Feng J, Liu T, Qin B, Zhang Y, Liu XS. 2012. Identifying ChIP-seq enrichment using MACS. *Nat Protoc* **7:** 1728–1740.

Hashizume R, Smirnov I, Liu S, Phillips JJ, Hyer J, McKnight TR, Wendland M, Prados M, Banerjee A, Nicolaides T, et al. 2012. Characterization of a diffuse intrinsic pontine glioma cell line: Implications for future investigations and treatment. *J Neurooncol* **110:** 305–313.

Heintzman ND, Hon GC, Hawkins RD, Kheradpour P, Stark A, Harp LF, Ye Z, Lee LK, Stuart RK, Ching CW, et al. 2009. Histone modifications at human enhancers reflect global cell-type-specific gene expression. *Nature* **459:** 108–112.

Henikoff S, Ahmad K. 2005. Assembly of variant histones into chromatin. *Annu Rev Cell Dev Biol* **21:** 133–153.

Langmead B, Trapnell C, Pop M, Salzberg SL. 2009. Ultrafast and memory-efficient alignment of short DNA sequences to the human genome. *Genome Biol* **10:** R25.

Li B, Carey M, Workman JL. 2007. The role of chromatin during transcription. *Cell* **128:** 707–719.

Louis DN, Ohgaki H, Wiestler OD, Cavenee WK, Burger PC, Jouvet A, Scheithauer BW, Kleihues P. 2007. The 2007 WHO classification of tumours of the central nervous system. *Acta Neuropathol* **114:** 97–109.

Margueron R, Reinberg D. 2011. The Polycomb complex PRC2 and its mark in life. *Nature* **469:** 343–349.

McCabe MT, Ott HM, Ganji G, Korenchuk S, Thompson C, Van Aller GS, Liu Y, Graves AP, Della Pietra A 3rd, Diaz E, et al. 2012. EZH2 inhibition as a therapeutic strategy for lymphoma with EZH2-activating mutations. *Nature* **492:** 108–112.

Plath K, Fang J, Mlynarczyk-Evans SK, Cao R, Worringer KA, Wang H, de la Cruz CC, Otte AP, Panning B, Zhang Y. 2003. Role of histone H3 lysine 27 methylation in X inactivation. *Science* **300:** 131–135.

Ransom M, Dennehey BK, Tyler JK. 2010. Chaperoning histones during DNA replication and repair. *Cell* **140:** 183–195.

Schwartzentruber J, Korshunov A, Liu XY, Jones DT, Pfaff E, Jacob K, Sturm D, Fontebasso AM, Quang DA, Tonjes M, et al. 2012. Driver mutations in histone H3.3 and chromatin remodelling genes in paediatric glioblastoma. *Nature* **482:** 226–231.

Simon JA, Kingston RE. 2009. Mechanisms of polycomb gene silencing: Knowns and unknowns. *Nat Rev Mol Cell Biol* **10:** 697–708.

Strahl BD, Allis CD. 2000. The language of covalent histone modifications. *Nature* **403:** 41–45.

Sturm D, Witt H, Hovestadt V, Khuong-Quang DA, Jones DT, Konermann C, Pfaff E, Tonjes M, Sill M, Bender S, et al. 2012. Hotspot mutations in H3F3A and IDH1 define distinct epigenetic and biological subgroups of glioblastoma. *Cancer Cell* **22:** 425–437.

Szenker E, Ray-Gallet D, Almouzni G. 2011. The double face of the histone variant H3.3. *Cell Res* **21:** 421–434.

Wong ET, Hess KR, Gleason MJ, Jaeckle KA, Kyritsis AP, Prados MD, Levin VA, Yung WK. 1999. Outcomes and prognostic factors in recurrent glioma patients enrolled onto phase II clinical trials. *J Clin Oncol* **17:** 2572–2578.

Wu G, Broniscer A, McEachron TA, Lu C, Paugh BS, Becksfort J, Qu C, Ding L, Huether R, Parker M, et al. 2012. Somatic histone H3 alterations in pediatric diffuse intrinsic pontine gliomas and non-brainstem glioblastomas. *Nat Genet* **44:** 251–253.

Yang W, Xia Y, Hawke D, Li X, Liang J, Xing D, Aldape K, Hunter T, Alfred Yung WK, Lu Z. 2012. PKM2 phosphorylates histone H3 and promotes gene transcription and tumorigenesis. *Cell* **150:** 685–696.

Zang C, Schones DE, Zeng C, Cui K, Zhao K, Peng W. 2009. A clustering approach for identification of enriched domains from histone modification ChIP-Seq data. *Bioinformatics* **25:** 1952–1958.

Zhang Y, Reinberg D. 2001. Transcription regulation by histone methylation: Interplay between different covalent modifications of the core histone tails. *Genes Dev* **15:** 2343–2360.